Research Square

Preprints are preliminary reports that have not undergone peer review.
They should not be considered conclusive, used to inform clinical practice,
or referenced by the media as validated information.

# Interactive ecotoxicity of co-exposure to 2-ethylhexyl diphenyl phosphate (EHDPP) and cadmium on wheat (Triticum aestivum L.) seedling growth in simulated agricultural soil adjacent to plastic recycling areas

**Chaoyi Wang**
**Wei Yin**
**Guangli Yan**
**Junxia Wang**
wangjunxia@usts.edu.cn

Suzhou University of Science and Technology School of Environmental Science and Engineering
https://orcid.org/0000-0001-6529-4001
**Xuedong Wang**

**Research Article**

**Keywords:** 2-Ethylhexyl diphenyl phosphate, Combined toxicity, Antagonistic effect, Wheat (Triticum aestivum L.) seedling, Photosynthesis

**Posted Date:** November 5th, 2026

**DOI:** https://doi.org/10.21203/rs.3.rs-11320552/v1

**License:** This work is licensed under a Creative Commons Attribution 4.0 International License.
Read Full License

# Abstract

### Aims

To determine the phytotoxicity of EHDPP, alone and co-contaminated with Cd, in wheat seedlings, and to identify the nature of their interaction, as reflected in growth, photosynthesis, antioxidant defense, and bioaccumulation.

### Methods

A pot experiment subjected wheat (*Triticum aestivum* L.) seedlings to three EHDPP levels (50, 500, 1,000 $ng \cdot g^{-1}$) and a combined EHDPP (500 $ng \cdot g^{-1}$) + Cd treatment. Biomass was weighed; photosynthesis was assessed via chlorophyll fluorescence ($F_v/F_m$, $F_v/F_0$) and pigment content; oxidative status via MDA and SOD, POD, CAT activities. Methods were spectrophotometry, kit assay and GC-MS; combined toxicity was evaluated by Abbott's formula and ANOVA with LSD tests.

### Results

EHDPP (50–1,000 $ng \cdot g^{-1}$) was phytotoxic to wheat seedlings, and co-exposure with Cd was mainly antagonistic. EHDPP alone reduced root, stem, and leaf biomass by 53%, 52%, and 38%, whereas Cd co-exposure raised biomass. Similarly, EHDPP decreased $F_v/F_m$ and $F_v/F_0$ by 4.62% and 41.16%, which Cd mitigated. Pigments increased but showed a biphasic response under combined stress, peaking at moderate EHDPP. MDA rose by 81% (EHDPP) and 97% (combined); under co-exposure, SOD peaked then fell, POD decreased with EHDPP, and CAT trended upward. EHDPP accumulated mainly in roots (RCFs 0.02–0.09); Cd raised RCFs but lowered TFs, enhancing root retention.

### Conclusions

EHDPP and Cd interact mainly antagonistically in wheat seedlings, modulating photosynthetic efficiency, oxidative balance, and contaminant distribution. This interaction, which shifts toxicity away from a simple additive response, is significant for the risk assessment of mixed-contaminated soils.


# Introduction

2-Ethylhexyldiphenyl phosphate (EHDPP) is widely used as a plasticizer and flame retardant in polyvinyl chloride (PVC), rubber, and food packaging (Green et al., 2008). EHDPP is an Organophosphate Esters (OPEs) that comprises of a benzene ring and an alkane (van der Veen and de Boer, 2012). As an additive to polymers, EHDPP does not chemically bind with products, making it easy to penetrate the environment during manufacturing, use, and handling (Wong et al., 2018). Elevated concentrations of EHDPP in soil may occur as a result of its extensive application scope combined with its physicochemical properties, a phenomenon attributable to its poor solubility in water (1.90 $mg \cdot L^{-1}$, 25°C) and high affinity for soil organic carbon (Koc = $7.38 \times 10^3$ $L \cdot Kg^{-1}$) (Fu et al., 2021).

Plastic waste generated by industrial and household production and consumption has increased significantly (Thompson et al., 2009). Improper disposal and unregulated treatment of plastic waste have resulted in widespread release of OPEs into the surrounding environment, with soil ultimately serving as the primary sink for these contaminants (Wan et al., 2016). Surface soil ΣOPEs levels at an open-pit recycling site in Tianjin stood at 122–2100 $ng \cdot g^{-1}$ (average: 829 $ng \cdot g^{-1}$), in stark contrast to the considerably lower concentrations detected at semi-closed recycling sites (58.5–316 ng/g; average: 138 $ng \cdot g^{-1}$) and farmland soils (37.7–156 $ng \cdot g^{-1}$; average: 65.2 $ng \cdot g^{-1}$) (Wang et al., 2020). Elevated Σ8OPEs contamination was evident in a plastic waste treatment area in Hebei Province, China, with an average concentration of 398 $ng \cdot g^{-1}$ (range: 38-1250 $ng \cdot g^{-1}$), whereas regional farmland exhibited substantially lower levels, averaging only 80 $ng \cdot g^{-1}$ (Wan et al., 2016). A growing body of evidence points to plastic waste recycling sites as significant hotspots of OPFR contamination. You et al. (2022) reported that the highest average concentration of EHDPP in high-altitude areas of Tibet was 44.45 $ng \cdot g^{-1}$. Analysis of surface soil samples collected near an e-waste recycling facility in northern Vietnam identified EHDPP at levels ranging between 2 and 67 $ng \cdot g^{-1}$ (Matsukami et al., 2015). EHDPP has been reported to be detected at high levels in soil, even exhibiting potential ecological risks.

In natural environments such as farmland systems, crops frequently encounter a range of simultaneous growth stresses. According to some reports, co-exposure to organic chemicals and heavy metals can significantly affect the uptake and translocation of organic chemicals in plants (Hu et al., 2021). In addition, studies have found that the migration capacity of hydrophobic polybrominated diphenyl ethers (PBDEs) into plant tissues is enhanced when they co-exist with polychlorinated biphenyls (PCBs) and heavy metals (Wang et al., 2011). On the other hand, copper, lead and chromium inhibit the uptake of polycyclic aromatic hydrocarbons by cabbages (Deng et al., 2018). Some researchers have also observed that copper addition can significantly promote the uptake of OPEs by plant roots (Hu et al., 2021). Among numerous heavy metals in soil, Cd has attracted considerable attention due to its high mobility, strong persistence and severe toxicity in the soil-plant system (Luo et al., 2026). Cadmium adversely affects chlorophyll synthesis, transpiration, and respiration, as well as stomatal opening, culminating in leaf chlorosis, dwarfism, growth suppression, and potentially plant death (Huybrechts et al., 2021). A close relationship exists between the photosynthetic system and the processes of OPE uptake and translocation in plants. Studies have demonstrated that exposure to tris(2-chloroethyl) phosphate (TCEP) can lead to alterations in the chlorophyll and carotenoid contents of wheat, thereby influencing photosynthetic activity (Liu et al., 2020). Despite extensive research on combined pollution in soil, studies specifically addressing the co-occurrence of OPEs and Cd in this matrix remain limited.

Among numerous crops, wheat has a strong capacity for Cd accumulation and has been widely used as an indicator plant for soil heavy-metal pollution (Zhang et al., 2026). As emerging organic pollutants, OPEs have attracted increasing attention regarding their uptake and translocation behaviors in wheat (Liu et al., 2026). In this regard, We simulated similar exposure concentrations of EHDPP in plastic recycling zones, added heavy metal Cd to simulate the complex OPFRs and heavy metal composite contamination state in the surrounding soil, using wheat as the indicator organism. By measuring wheat

chlorophyll fluorescence parameters, photosynthetic pigments, oxidative stress, and other indicators, we described the plant toxicity of EHDPP and Cd, and used a combined correlation formula to calculate and analyze the interaction between EHDPP and Cd.

# Materials and Methods

Chemicals and Reagents

Details of the chemicals used in this research are shown in **Text S1**

Pot experiments

Simulated soil for potted plants was collected from the topsoil (0–20 cm) on the campus of Suzhou University of Science and Technology, air-dried, ground, and sieved (2 mm) (Table 1).

Wheat seeds were disinfected with 3% hydrogen peroxide for 0.5 h, rinsed three times, soaked in deionized water for at least 6 h, and then incubated in the dark at 20°C for 48 h for germination. After 7 d of growth, the wheat reached the three-leaf stage. Six seedlings were transplanted into each pot, with cultivation temperatures maintained at 20-22°C, humidity at approximately 70%, a light cycle of 16 h:8 h (light : dark), and a light intensity of 250 μmol $m^{-2}s^{-1}$. All experimental groups were supplied with 100 ml of 1/4 Hoagland nutrient solution once a week to replenish water and nutrients.

Table 1
Soil parameters in the pot experiments

| Parameters | pH | Organic matter content ($g \cdot kg^{-1}$) | Alkali-hydrolytic nitrogen content ($mg \cdot kg^{-1}$) | Available phosphorus content ($mg \cdot kg^{-1}$) | Available potassium content ($mg \cdot kg^{-1}$) | Total content of Cd ($mg \cdot kg^{-1}$) |
|---|---|---|---|---|---|---|
| Values | 5.78 | 31.05 | 109.40 | 84.80 | 56.20 | 0.05 |

Soil contamination: Mix an appropriate concentration of EHDPP powder with pre-treated soil (dry weight, DW) mechanically to ensure uniform distribution. Obtain soils with different concentrations of EHDPP contamination (0, 100, 200, 500, 1000 $\mu g \cdot kg^{-1}$). At the same time, apply cadmium ($CdCl_2$) aqueous solution to the soil, with Cd concentrations of 0.05 and 0.5 $mg \cdot kg^{-1}$. After 30 d of cultivation, collect wheat seedlings, wash them with deionized water, blot dry with filter paper, and measure fresh weight, root length, and shoot length. Subsequently, divide the wheat seedlings into shoots and roots. Part of the leaves is used to determine photosynthetic pigment content, chlorophyll fluorescence effect, soluble protein, and lipid content, while another part is used to determine the activities of superoxide dismutase, peroxidase, catalase, and malondialdehyde content in leaves and roots. The remaining roots and shoots are used to measure EHDPP content.

Determination of physiological indicators of wheat

This study adopted published classical and modified methods to systematically determine photosynthetic characteristics (chlorophyll fluorescence and photosynthetic pigments), soluble protein, lipid/carbohydrate contents, antioxidant enzyme activities, and EHDPP in wheat seedlings via spectrophotometry, kit assay and GC-MS detection. The detailed procedures are presented in **Text S2**.

Data Processing and statistic analysis

The combined toxic effect of EHDPP and Cd was calculated using Abbott's formula (Liu et al., 2019a). The formula is as follows

$$C_{exp}=(A+B\text{-}A\times B)/100$$

1

$$RI=OB/C_{exp}$$

2

where A and B represent the degree of inhibition caused by the individual exposure substances, each expressed as the rate of change in the endpoint relative to the blank control group. The OB (Observed Inhibition) value denotes the rate of change in the endpoint under combined exposure. $C_{exp}$ is considered the calculated combined effect, and RI represents the ratio of the actually observed value to $C_{exp}$. An interaction type is classified as antagonistic when RI < 1, and synergistic when RI > 1.3

The experimental results were analyzed statistically using ANOVA, and the differences between groups were analyzed using the LSD method and a significant difference is considered at the 0.05 level ($P < 0.05$).

# Results

Biomass responses of wheat to EHDPP single and Cd-combined stress

The dry weights of roots, stems, and leaves of wheat seedlings were determined for all treatment groups. As shown in Fig. 1, the dry weights under single EHDPP exposure were consistently lower than those of the unexposed control group, and the dry weights of roots, stems, and leaves decreased with increasing EHDPP exposure concentrations. Compared to the blank control, root dry weight decreased by 24%, 26%, 38%, and 53%; stem dry weight decreased by 31%, 33%, 42%, and 52%; and leaf dry weight decreased by 15%, 31%, 37%, and 38% under the four EHDPP exposure concentrations, respectively. Compared to the single Cd treatment group, dry weights in the combined treatment groups increased in most cases, with the exceptions of stem and leaf dry weights in the 500 + 500 ng/g treatment group and leaf dry weight in the 1000 + 500 $ng{\cdot}g^{-1}$ treatment group, which were lower. When compared to the corresponding single EHDPP treatment concentrations, only stem dry weight exhibited an increasing trend in the combined treatment groups.

PSII photochemical efficiency of wheat under EHDPP single and Cd-combined stress

Figure 2 presents the Maximum photochemical quantum yield ($F_v/F_m$) and potential photochemical quantum yield ($F_v/F_0$) values of wheat seedlings. Both $F_v/F_m$ and $F_v/F_0$ decreased with increasing EHDPP exposure concentrations. Compared to the control, $F_v/F_m$ decreased by 3.87%, 4.06%, 4.11%, and 4.62%, while $F_v/F_0$ exhibited a more pronounced reduction, decreasing by 25.87%, 27.59%, 27.51%, and 41.16%, respectively.

After the addition of Cd as a co-contaminant, $F_v/F_m$ and $F_v/F_0$ values were found to increase. Notably, in the combined exposure group of 1000 $ng \cdot g^{-1}$ EHDPP with Cd, $F_v/F_m$ and $F_v/F_0$ increased significantly compared to single EHDPP exposure at the same concentration ($p < 0.05$).

Photosynthetic pigment responses of wheat under EHDPP single and Cd-combined stress

Changes in chlorophyll concentration are widely used as an indicator of the photosynthetic status of plants under external environmental stress (Pattanayak and Tripathy, 2011).

Figure 3 illustrates the variations in the contents of three photosynthetic pigments in wheat under different treatments. The contents of all three photosynthetic pigments were found to be higher than those in the control group. With increasing EHDPP exposure concentrations, the contents of chlorophyll a and carotenoids exhibited an upward trend, whereas chlorophyll b content initially showed an increasing trend but began to decrease significantly when the EHDPP concentration reached 500 $ng \cdot g^{-1}$.

In the combined treatment groups, the contents of the three photosynthetic pigments initially increased and then decreased with increasing EHDPP contamination concentrations, suggesting that chlorophyll a and carotenoids exhibited higher sensitivity compared to single EHDPP exposure. This indicates that the combined contamination of EHDPP and Cd had a more pronounced effect on photosynthesis in wheat. When comparing the combined treatment groups with the single Cd treatment, chlorophyll a and chlorophyll b contents were significantly reduced only in the combined treatment groups at EHDPP concentrations of 500 $ng \cdot g^{-1}$ and 1000 $ng \cdot g^{-1}$, whereas carotenoid content exhibited an overall increasing trend.

Oxidative stress and antioxidant enzyme responses of wheat under EHDPP single and Cd-combined stress

To investigate the oxidative damage and the response of the antioxidant defense system in wheat under EHDPP exposure, both alone and in combination with Cd, we measured the malondialdehyde (MDA) content and the activities of several antioxidant enzymes, including superoxide dismutase (SOD), peroxidase (POD), and catalase (CAT), as shown in Fig. 4.

As presented in Fig. 4A, MDA content increased in all treatment groups compared to the uncontaminated control. Specifically, MDA content increased by 41%, 59%, 72%, and 81% under single EHDPP treatments,

and by 74%, 80%, 89%, and 97% in the EHDPP + Cd combined treatment groups, respectively. Comparison between single EHDPP treatments and combined treatments revealed that MDA content was higher in all combined treatment groups, with increases of 23%, 13%, 9%, and 9% relative to the corresponding single EHDPP treatments.

The activities of SOD, POD, and CAT under different treatments are presented in Fig. 4 **(B-D)**. Under single EHDPP stress, SOD activity increased significantly with increasing concentration, POD activity increased with increasing concentration, and CAT activity initially increased and then decreased with increasing concentration.

In the combined treatment groups, SOD activity was significantly higher than that in the uncontaminated control across all treatments; however, the overall trend showed an initial increase followed by a decline at the highest combined concentration. At the highest combined concentration, SOD activity decreased by 11% compared to the corresponding single EHDPP treatment. POD activity in the combined treatment groups decreased with increasing EHDPP concentration. Relative to the single EHDPP treatment, POD activity increased at the lowest combined concentration but decreased at all other combined concentrations. In contrast to the single EHDPP treatments, where CAT activity gradually decreased with increasing concentration, CAT activity in the combined treatment groups initially increased and then decreased. Moreover, when comparing combined and single treatments at the same EHDPP concentrations, CAT activity decreased only at the lowest concentration but increased in all other combined treatment groups.

Effects of EHDPP and Cd single and combined stresses on lipids and soluble proteins in wheat

As shown in Fig. 5, single EHDPP stress significantly decreased both lipid and soluble protein contents in wheat. Under single EHDPP exposure, lipid content gradually declined from 3.48% in the control to 3.12%, 3.03%, 3.05%, and 2.90% at EHDPP concentrations of 100, 200, 500, and 1000 ng·g⁻¹, respectively, representing decreases of 10.3%, 12.9%, 12.4%, and 16.7% relative to the uncontaminated control. A more pronounced reduction was observed for soluble protein, which decreased from 203 $\mu g \cdot g^{-1}$ in the control to 162, 144, 132, and 115 $\mu g \cdot g^{-1}$ across the same concentration gradient, corresponding to decreases of 20.2%, 29.1%, 35.0%, and 43.3%, respectively.

In the EHDPP + Cd combined treatment groups, lipid content consistently increased compared with the corresponding single EHDPP treatments, rising by approximately 4%, 7%, 2%, and 6% at 100, 200, 500, and 1000 $ng \cdot g^{-1}$ EHDPP, respectively. This suggests that Cd co-exposure partially alleviated the lipid depletion caused by EHDPP alone. For soluble protein, the response to Cd co-exposure was concentration-dependent: at the lowest combined concentration (100 $ng \cdot g^{-1}$ EHDPP + Cd), soluble protein content decreased further to approximately 120 $\mu g \cdot g^{-1}$ (vs. 162 $\mu g \cdot g^{-1}$ under single EHDPP), whereas at all higher combined concentrations (200–1000 $ng \cdot g^{-1}$ EHDPP + Cd), soluble protein content was higher than in the corresponding single EHDPP treatments, reaching approximately 150, 142, and 123 $\mu g \cdot g^{-1}$, respectively.

Absorption and translocation of EHDPP in wheat under different treatments

We determined the EHDPP concentrations in the roots, stems, and leaves of wheat (**Fig. S1**). The results showed that EHDPP predominantly accumulated in the roots, with concentrations decreasing progressively during upward translocation to the aerial parts. Under combined exposure to EHDPP and Cd, EHDPP concentrations in the roots, stems, and leaves were lower compared to those under single EHDPP exposure. For instance, in the roots, EHDPP concentrations under combined exposure decreased by 8%, 12%, 17%, and 38%, respectively, relative to single exposure.

The root concentration factor (RCF) and translocation factor (TF) are shown in Fig. 6**(A-B)**. Under single EHDPP exposure, RCF values decreased from 0.093 to 0.021 as EHDPP concentration increased from 100 to 1000 ng·g⁻¹, whereas TF values increased from 0.064 to 0.252 over the same concentration range. Cd co-exposure increased RCF values at all EHDPP concentrations (e.g., 0.102 vs. 0.093 at 100 $ng \cdot g^{-1}$; 0.036 vs. 0.021 at 1000 $ng \cdot g^{-1}$) but decreased TF values (e.g., 0.050 vs. 0.064 at 100 $ng \cdot g^{-1}$; 0.208 vs. 0.252 at 1000 $ng \cdot g^{-1}$). The regression analysis (Fig. 6C) showed a significant negative correlation between RCF and TF under both single ($R^2 = 0.952$) and combined ($R^2 = 0.911$) exposure.

## Discussions

# Interactive effects of EHDPP and Cd on wheat growth and photosynthetic performance

Dry biomass accumulation of roots, stems and leaves is the most direct endpoint for evaluating phytotoxic responses to combined pollution stress. In the present study, cross-treatment comparison showed that root, stem and leaf dry weights under combined EHDPP and Cd exposure were generally higher than those under single Cd treatment, and the combined toxicity assessment (**Fig. S2**) confirmed antagonistic interactions between EHDPP and Cd on dry weight across all three wheat tissues.

The observed growth responses are intrinsically driven by changes in plant photosynthetic performance, which is highly sensitive to abiotic stress. As a core indicator of PSII function, the maximum quantum efficiency of PSII (Fv/Fm) has been widely reported to decline significantly under exposure to both heavy metals and organophosphorus flame retardants (OPFRs). Previous studies have documented that Fv/Fm of the marine diatom Chaetoceros muelleri first increased and then decreased with rising triphenyl phosphate (TPhP) concentrations, with 3.2 $mg \cdot L^{-1}$ TPhP causing severe photosynthetic impairment after 96 h of high-light exposure (Wang et al., 2021). Similarly, Fv/Fm of the freshwater green alga Chlorella sorokiniana decreased progressively with increasing concentrations of tetrabromobisphenol A (TBBPA), tris(1,3-dichloro-2-propyl) phosphate (TDCPP), and tributyl phosphate (TBP) (Liu et al., 2023). In our study, combined toxicity assessment (**Fig. S3**) showed that EHDPP and Cd exerted antagonistic effects on wheat Fv/Fm across nearly all tested concentrations. The interaction was synergistic only for the $Fv/F_0$ parameter at the lowest exposure concentration, and remained antagonistic at all higher concentrations. Such antagonistic modulation of phytotoxicity between OPFRs and co-occurring

pollutants has been previously documented: for example, polystyrene microplastics were reported to mitigate the inhibitory effect of TPhP on algal photosynthesis, producing a net antagonistic combined toxicity outcome (Wang et al., 2021), which aligns closely with the observations in the present study.

Variations in photosynthetic performance are further supported by changes in photosynthetic pigment pools, which directly mediate light harvesting and photoprotection. Prior work has shown that chlorophyll a content in wheat increases under low-concentration chlorinated OPFR exposure (< 0.1 $\mu mol \cdot L^{-1}$) and begins to decline only when concentrations exceed this threshold, while chlorophyll b content decreases progressively with rising OPFR levels, and carotenoid content remains significantly elevated relative to controls across all treatments (Liu et al., 2020). Consistent with these observations, TDCPP exposure was reported to increase chlorophyll content in Chlorella sorokiniana (Liu et al., 2023), and TCIPP elevated total chlorophyll content in pak choi (Luo et al., 2021). These responses reflect an adaptive self-protective strategy: under mild external or oxidative stress, plants upregulate chlorophyll synthesis to enhance light energy capture, while elevated carotenoid content acts as an antioxidant defense to scavenge reactive oxygen species (ROS) and protect the photosynthetic apparatus from oxidative damage (Shen et al., 2017, 2019). In the present study, combined toxicity assessment (**Fig. S4**) indicated that the EHDPP-Cd interaction on chlorophyll a was synergistic only at the lowest concentration and antagonistic across all higher concentrations, while interactions on chlorophyll b and carotenoid content were antagonistic at all tested concentration levels.

Collectively, the consistent patterns across dry biomass, chlorophyll fluorescence parameters and photosynthetic pigment pools provide convergent evidence that, over the tested concentration range, co-exposure to EHDPP does not exacerbate Cd-induced phytotoxicity; instead, the dominant antagonistic interaction alleviates Cd-mediated suppression of wheat growth and photosynthetic function.

## Oxidative stress response and antioxidant defense adaptation of wheat under EHDPP and Cd co-exposure

Excess reactive oxygen species (ROS) can induce lipid peroxidation in cells (Li et al., 2015), and malondialdehyde (MDA), as a stable end-product of lipid peroxidation (Xia et al., 2015), serves as a sensitive diagnostic indicator of oxidative stress and cellular damage (Yin et al., 2007). Previous studies have consistently reported MDA elevation in biota exposed to organophosphate flame retardants (OPFRs): Liu et al. (2023) showed that MDA content in *Chlorella sorokiniana* increased with rising concentrations of TDCPP and TBP, while Luo et al. (2021) found that MDA content in pak choi increased under high-concentration TCIPP exposure, although the increase was not significant at low concentrations (< 500 $ng \cdot g^{-1}$). In the present study, the combined toxicity assessment (**Fig. S5**) indicated that EHDPP and Cd exhibited a synergistic interaction on MDA content at the lowest concentration, but switched to antagonistic interactions at all other concentrations. This concentration-dependent transition suggests that at low doses the two pollutants jointly amplify membrane lipid

damage, whereas at elevated levels their effects partially offset each other—possibly reflecting suppressed uptake or metabolic competition between EHDPP and Cd.

To counteract oxidative damage, plants activate an enzymatic antioxidant defense system in which superoxide dismutase (SOD) is recognized as the first line of defense, catalyzing the conversion of superoxide anions ($\cdot O_2^-$) into less toxic $H_2O_2$ and $O_2$; catalase (CAT) and peroxidase (POD) subsequently scavenge $H_2O_2$ by catalyzing its disproportionation into harmless $O_2$ and $H_2O$ (Zhang et al., 2016). This "low-concentration induction, high-concentration inhibition" pattern has been widely documented. Wan et al. (2016) reported that POD, SOD, and CAT activities in wheat peaked at an OPFR concentration of 100 $\mu g \cdot L^{-1}$ and declined sharply thereafter. Luo et al. (2021) observed a similar hormetic trend for SOD, POD, and CAT in pak choi with increasing TCIPP concentrations. Likewise, Liu et al. (2023) found that when TDCPP reached 50 $mg \cdot L^{-1}$, SOD activity no longer increased but dropped sharply to 589.70 $U \cdot g^{-1}$; in their earlier work on *Phaeodactylum tricornutum* exposed to TBP, SOD and CAT activities decreased progressively with prolonged exposure time, although SOD levels in all treatment groups remained above those of the control (Liu et al., 2019b). Consistent with these reports, the present results can be interpreted as follows: under low-concentration EHDPP stress, the elevated activities of SOD, POD, and CAT represent a direct adaptive response to scavenge ROS generated by abiotic stress; under high-concentration EHDPP stress, however, the decline in enzyme activities indicates that the scavenging capacity is insufficient and the antioxidant defense system becomes overwhelmed by excess ROS (Chen et al., 2018).

Overall, the antioxidant defense response of wheat to EHDPP and Cd co-exposure is a complex, dose-dependent process. The combined toxicity assessment (**Fig. S5**) revealed that EHDPP and Cd exerted predominantly antagonistic effects on SOD and POD activities, whereas CAT activity showed a synergistic interaction at the lowest concentration and antagonistic interactions at all higher concentrations. These enzyme-specific and concentration-dependent interaction patterns imply that different antioxidant defense arms respond divergently to the joint stress, and that antagonism generally intensifies with exposure level.

As osmoprotectants, soluble proteins and lipids are also sensitive to external stress, and soluble protein content tends to decline once plants suffer irreversible damage (Huang et al., 2014). Liang et al. (2020) reported that soluble protein content in wheat initially increased and then decreased with rising sodium benzoate concentrations under heavy metal co-stress, reflecting an initial osmotic adjustment followed by structural degradation. In the present study, the combined toxicity assessment (**Fig. S6**) showed that EHDPP and Cd exhibited predominantly antagonistic interactions on both lipid and soluble protein contents in wheat.

## Uptake, translocation and accumulation of EHDPP in wheat as modulated by co-exposure to Cd

In the present study, the accumulation of EHDPP in wheat was relatively low, which may be attributed to its high hydrophobicity and chemical structure. For comparison, Luo et al. (2021) detected TCIPP concentrations of 170.6, 48.7, and 890.1 $\mu g \cdot kg^{-1}$ in the roots, stems, and leaves of pak choi, respectively, at an exposure concentration of 1000 $\mu g \cdot kg^{-1}$—substantially higher than the EHDPP levels observed in the present study. This discrepancy likely reflects differences in both plant species and compound hydrophobicity, as discussed below.

The root concentration factor (RCF) values obtained here were comparable to those reported by Hu et al. (2021) for maize and tomato. Notably, RCF exhibited a decreasing trend with increasing EHDPP exposure concentrations, consistent with the findings of Shen et al. (2019). The translocation factor (TF) values of EHDPP in wheat were slightly higher than those reported by Hu et al. (2021), but substantially lower than the TF values of TCIPP (log Kow = 2.89) in pak choi (Luo et al., 2021). Since the RCF values consistently exceeded the TF values, EHDPP clearly tends to accumulate preferentially in wheat roots rather than being translocated upward to shoots. This pattern can be explained by the combined effects of hydrophobicity and transpiration-driven mass flow: transpiration serves as the primary driving force for the upward translocation of neutral organic compounds, and chemicals with log Kow values between 0.5 and 3.0 can readily cross the Casparian strip and enter shoots via the transpiration stream, whereas more hydrophobic compounds tend to be retained in undeveloped root tips or bound to proteins in the xylem sap (Burken and Schnoor, 1998; Wu et al., 2022). Previous studies have likewise shown that highly hydrophobic OPEs are translocated less efficiently than their less hydrophobic counterparts (Wan et al., 2016; Wan et al., 2017).

Beyond the intrinsic properties of EHDPP, heavy metal co-exposure can significantly alter the uptake and translocation of organic pollutants in plants. Hu et al. (2021) found that Cu increased EHDPP concentrations in plant roots and shoots by 80.9% and 52.8%, respectively. Deng et al. (2018) reported that Cd slightly enhanced polycyclic aromatic hydrocarbon (PAH) accumulation in Chinese cabbage roots but decreased PAH content in the stems—a pattern similar to that observed in the present study. Given that both EHDPP and PAHs are persistent organic pollutants with log Kow > 3, Cd may enhance their root uptake through a common mechanism (Zhang et al., 2017).

Two complementary mechanisms may account for the heavy-metal-facilitated root accumulation. First, heavy metals can damage root structures—including root diameter, volume, surface area, root tips, cell membranes, and junction zones (Deng et al., 2018; Pätsikkä et al., 2002)—thereby weakening the root exclusion barrier, increasing cell membrane permeability, and disrupting the Casparian strip. This structural compromise enables hydrophobic compounds to enter damaged roots non-selectively via the apoplastic pathway (Chen et al., 2020; Luo et al., 2015). For instance, Cu exposure induced root damage and electrolyte leakage in maize, enhancing the passive penetration of polybrominated diphenyl ethers (PBDEs) into root cells (Wan et al., 2016; Wang et al., 2016). Second, from a chemical interaction perspective, EHDPP is classified as an electron-cyclic substituted OPE (EC-OPE); its electron-rich aromatic structure can coordinate strongly with metal ions, favoring the formation of metal–EHDPP chelates and thereby promoting their uptake into roots (Hu et al., 2021). Together, these physical and

chemical pathways explain why Cd co-exposure modulates the uptake and translocation of EHDPP in wheat.

## Conclusions

This study demonstrates that the combined stress of EHDPP and Cd elicits predominantly antagonistic interactions across multiple physiological and biochemical endpoints in wheat, including biomass, photosynthetic pigment content, oxidative stress markers, and reserve substance levels, with synergistic effects restricted to a narrow subset of sensitive parameters ($F_v/F_o$, chlorophyll a, MDA, and CAT) exclusively at the lowest combined concentration. Notably, Cd co-exposure enhanced root retention of EHDPP while impeding its upward translocation. These findings reveal a strong concentration-dependent complexity in the joint toxicity of organic phosphate esters and heavy metals, challenging the assumption of simple additive effects and underscoring the necessity of evaluating contaminant interactions across a realistic concentration spectrum. Within the broader field of mixed pollutant toxicology, this work provides critical empirical evidence for the largely underexplored combined phytotoxicity of emerging organic flame retardants and ubiquitous metal contaminants in staple crops. A limitation of the experimental design is the restricted number of fixed-ratio concentration combinations, which precludes the construction of a full concentration–response surface and mechanistic resolution of the observed interaction modes, particularly the antagonistic-to-synergistic shift at low doses. Future studies integrating transcriptomic or metabolomic approaches with a wider concentration matrix are warranted to elucidate the molecular underpinnings of these complex interactions and to validate their environmental relevance under field conditions.

## Declarations

# CRediT authorship contribution statement

**Chaoyi Wang:** Writing – original draft, Methodology, Formal analysis, Data curation. **Wei Yin:** Validation, Conceptualization, Methodology, Data curation. **Guangli Yan:** Formal analysis**,** Validation. **Junxia Wang:** Writing – review & editing, Supervision, Funding acquisition, Formal analysis, Conceptualization. **Xuedong Wang:** Funding acquisition, Resources

# Acknowledgments

The research received collaborative support from the Suzhou National Joint Laboratory focused on Green and Low-carbon Wastewater Treatment and Resource Utilization Technology (SZLSDT202404) and Suzhou Science and technology to strengthen agriculture innovation project (SNG2020050).

# Declare of competing interest

On behalf of all the authors, the corresponding author states that no conflicts of interest exist.

# References


1. Bradford MM (1976) A rapid and sensitive method for the quantitation of microgram quantities of protein utilizing the principle of protein-dye binding. Anal Biochem 72:248–254
2. Burken JG, Schnoor JL (1998) Predictive Relationships for Uptake of Organic Contaminants by Hybrid Poplar Trees. Environ Sci Technol 32:3379–3385
3. Chen J, Saleem M, Wang C, Liang W, Zhang Q (2018) Individual and combined effects of herbicide tribenuron-methyl and fungicide tebuconazole on soil earthworm Eisenia fetida. Sci Rep 8:2967
4. Chen J, Xia X, Chu SQ, Wang H, Gan JJ (2020) Cation-π Interactions with Coexisting Heavy Metals Enhanced the Uptake and Accumulation of Polycyclic Aromatic Hydrocarbons in Spinach. Environ Sci Technol 54:7261–7270
5. Deng S, Ke T, Wu Y, Zhang C, Hu Z, Yin H, Guo L, Chen L, Zhang D (2018) Heavy Metal Exposure Alters the Uptake Behavior of 16 Priority Polycyclic Aromatic Hydrocarbons (PAHs) by Pak Choi (Brassica chinensis L). Environ Sci Technol 52:13457–13468
6. Fu J, Fu K, Chen Y, Li X, Ye T, Gao K, Pan W, Zhang A, Fu J (2021) Long-Range Transport, Trophic Transfer, and Ecological Risks of Organophosphate Esters in Remote Areas. Environ Sci Technol 55:10192–10209
7. Green N, Schlabach M, Bakke T, Brevik E, Dye C, Herzke D, Huber S, Plosz B, Remberger M, Schøyen M, Uggerud H, Vogelsang C (2008) SCREENING OF SELECTED METALS AND NEW ORGANIC CONTAMINANTS 2007
8. Hu B, Jiang L, Zheng Q, Luo C, Zhang D, Wang S, Xie Y, Zhang G (2021) Uptake and translocation of organophosphate esters by plants: Impacts of chemical structure, plant cultivar and copper. Environ Int 155:106591
9. Huang C, Wei G, Jie Y, Wang L, Zhou H, Ran C, Huang Z, Jia H, Anjum SA (2014) Effects of concentrations of sodium chloride on photosynthesis, antioxidative enzymes, growth and fiber yield of hybrid ramie. Plant Physiol Biochem 76:86–93
10. Huybrechts M, Hendrix S, Kyndt T, Demeestere K, Vandamme D, Cuypers A (2021) Short-term effects of cadmium on leaf growth and nutrient transport in rice plants. Plant Sci 313:111054
11. Li F, Liang Z, Zheng X, Zhao W, Wu M, Wang Z (2015) Toxicity of nano-$TiO_2$ on algae and the site of reactive oxygen species production. Aquat Toxicol 158:1–13
12. Li H, Sheng G, Chiou CT, Xu O (2005) Relation of Organic Contaminant Equilibrium Sorption and Kinetic Uptake in Plants. Environ Sci Technol 39:4864–4870
13. Liang P-p, Zhao C, Lin Y, Geng J-j, Chen Y, Chen D-h, Zhang X (2020) Effects of sodium benzoate on growth and physiological characteristics of wheat seedlings under compound heavy metal stress. J Integr Agr 19:1010–1018

14. Lichtenthaler HK (1987) Chlorophylls and carotenoids: Pigments of photosynthetic biomembranes. Methods in Enzymology. Academic, pp 350–382
15. Liu D, Qv M, Dai D, Wang X, Zhu L (2023) Toxic responses of freshwater microalgae Chlorella sorokiniana due to exposure of flame retardants. Chemosphere 310:136808
16. Liu N, Zhong G, Zhou J, Liu Y, Pang Y, Cai H, Wu Z (2019a) Separate and combined effects of glyphosate and copper on growth and antioxidative enzymes in Salvinia natans (L.) All. Sci Total Environ 655:1448–1456
17. Liu Q, Liu M, Wu S, Xiao B, Wang X, Sun B, Zhu L (2020) Metabolomics Reveals Antioxidant Stress Responses of Wheat (Triticum aestivum L.) Exposed to Chlorinated Organophosphate Esters. J Agric Food Chem 68:6520–6529
18. Liu Q, Tang X, Wang Y, Yang Y, Zhang W, Zhao Y, Zhang X (2019b) ROS changes are responsible for tributyl phosphate (TBP)-induced toxicity in the alga Phaeodactylum tricornutum. Aquat Toxicol 208:168–178
19. Liu S, Xue H, Wang G, Wang Y, Hou J, Zhang J, Wang H, Liu Y (2026) Influence of nitrate on uptake and translocation of organophosphate esters in wheat (Triticum aestivum L). Environ Pollut 395:127807
20. Luo C, Wang S, Wang Y, Yang R, Zhang G, Shen Z (2015) Effects of EDDS and plant-growth-promoting bacteria on plant uptake of trace metals and PCBs from e-waste-contaminated soil. J Hazard Mater 286:379–385
21. Luo Q, Li Y, Wu Z, Wang X, Wang C, Shan Y, Sun L (2021) Phytotoxicity of tris-(1-chloro-2-propyl) phosphate in soil and its uptake and accumulation by pakchoi (Brassica chinensis L. cv. SuZhou) Chemosphere 277:130347
22. Luo Z, Ma J, Cao Y, Xu Y, Ma C, Wang J, Yan W (2026) Silicon nanoparticles promote soybean growth in Cd-contaminated soil by modulating soil bacterial networks. Appl Soil Ecol 226:107373
23. Matsukami H, Tue NM, Suzuki G, Someya M, Tuyen LH, Viet PH, Takahashi S, Tanabe S, Takigami H (2015) Flame retardant emission from e-waste recycling operation in northern Vietnam: Environmental occurrence of emerging organophosphorus esters used as alternatives for PBDEs. Sci Total Environ 514:492–499
24. Pätsikkä E, Kairavuo M, Šeršen F, Aro E-M, Tyystjärvi E (2002) Excess Copper Predisposes Photosystem II to Photoinhibition in Vivo by Outcompeting Iron and Causing Decrease in Leaf Chlorophyll. Plant Physiol 129:1359–1367
25. Pattanayak GK, Tripathy BC (2011) Overexpression of Protochlorophyllide Oxidoreductase C Regulates Oxidative Stress in Arabidopsis. PLoS ONE 6:e26532
26. Santín G, Eljarrat E, Barceló D (2016) Simultaneous determination of 16 organophosphorus flame retardants and plasticizers in fish by liquid chromatography-tandem mass spectrometry. J Chromatogr A 1441:34–43
27. Shen Y, Li J, Gu R, Yue L, Zhan X, Xing B (2017) Phenanthrene-triggered Chlorosis is caused by elevated Chlorophyll degradation and leaf moisture. Environ Pollut 220:1311–1321

28. Shen Y, Li J, Shi S, Gu R, Zhan X, Xing B (2019) Application of carotenoid to alleviate the oxidative stress caused by phenanthrene in wheat. Environ Sci Pollut Res 26:3593–3602
29. Thompson RC, Moore CJ, vom Saal FS, Swan SH (2009) Plastics, the environment and human health: current consensus and future trends. Philos Trans R Soc Lond B Biol Sci 364:2153–2166
30. van der Veen I, de Boer J (2012) Phosphorus flame retardants: Properties, production, environmental occurrence, toxicity and analysis. Chemosphere 88:1119–1153
31. Wan W, Huang H, Lv J, Han R, Zhang S (2017) Uptake, Translocation, and Biotransformation of Organophosphorus Esters in Wheat (Triticum aestivum L). Environ Sci Technol 51:13649–13658
32. Wan W, Zhang S, Huang H, Wu T (2016) Occurrence and distribution of organophosphorus esters in soils and wheat plants in a plastic waste treatment area in China. Environ Pollut 214:349–353
33. Wang SC, Gao ZY, Liu FF, Chen SQ, Liu GZ (2021) Effects of polystyrene and triphenyl phosphate on growth, photosynthesis and oxidative stress of Chaetoceros meülleri. Sci Total Environ 797:149180
34. Wang S, Wang Y, Luo C, Jiang L, Song M, Zhang D, Wang Y, Zhang G (2016) Could Uptake and Acropetal Translocation of PBDEs by Corn Be Enhanced Following Cu Exposure? Evidence from a Root Damage Experiment. Environ Sci Technol 50:856–863
35. Wang S, Zhang S, Huang H, Zhao M, Lv J (2011) Uptake, translocation and metabolism of polybrominated diphenyl ethers (PBDEs) and polychlorinated biphenyls (PCBs) in maize (Zea mays L). Chemosphere 85:379–385
36. Wang X, Zhu Q, Yan X, Wang Y, Liao C, Jiang G (2020) A review of organophosphate flame retardants and plasticizers in the environment: Analysis, occurrence and risk assessment. Sci Total Environ 731:139071
37. Wong F, de Wit CA, Newton SR (2018) Concentrations and variability of organophosphate esters, halogenated flame retardants, and polybrominated diphenyl ethers in indoor and outdoor air in Stockholm, Sweden. Environ Pollut 240:514–522
38. Wu J-y, Zhu T, Chen Z-m, Guo J-s, Hou X-y, Wang D-r, Zhang L-x, Gao J-m (2022) Occurrence, seasonal variation, potential sources, and risks of organophosphate esters in a cold rural area in Northeast China. Sci Total Environ 834:155361
39. Xia B, Chen B, Sun X, Qu K, Ma F, Du M (2015) Interaction of $TiO_2$ nanoparticles with the marine microalga Nitzschia closterium: Growth inhibition, oxidative stress and internalization. Sci Total Environ 508:525–533
40. Yin Y, Jia H, Sun Y, Yu H, Wang X, Wu J, Xue Y (2007) Bioaccumulation and ROS generation in liver of Carassius auratus, exposed to phenanthrene. Comp Biochem Physiol C: Toxicol Pharmacol 145:288–293
41. You J, Chen ZM, Hou XY, Guo JS, Wang CC, Gao JM (2022) Occurrence, potential sources and risks of organophosphate esters in the high-elevation region, Tibet, China. Sci Total Environ 806:151348
42. Zhang L, Zhao N, Sarmah AK, Zhao L, Zeng Q, La Y, Lin D, Wang R (2026) 3-Mercaptopropyltrimethoxysilane combined with manganese sulfate reduces Cd accumulation in wheat on weakly alkaline soils via plant-soil-microorganism regulation. J Environ Sci, 105575

43. Zhang S, Yao H, Lu Y, Yu X, Wang J, Sun S, Liu M, Li D, Li Y-F, Zhang D (2017) Uptake and translocation of polycyclic aromatic hydrocarbons (PAHs) and heavy metals by maize from soil irrigated with wastewater. Sci Rep 7:12165
44. Zhang Y, Zhang H, Sun X, Wang L, Du N, Tao Y, Sun G, Erinle KO, Wang P, Zhou C, Duan S (2016) Effect of dimethyl phthalate (DMP) on germination, antioxidant system, and chloroplast ultrastructure in Cucumis sativus L. Environ Sci Pollut Res 23:1183–1192
45. Zhu J, Lu J, Xu X, Huang Y, Li W, Gu Y, Zheng H, Jiang C, Cheng T, Tian Y, Zhu Y, Cao W, Yao X (2026) Estimating leaf net photosynthetic rate in wheat using sun-induced chlorophyll fluorescence. Smart Agricultural Technol 15:102444

# Figures

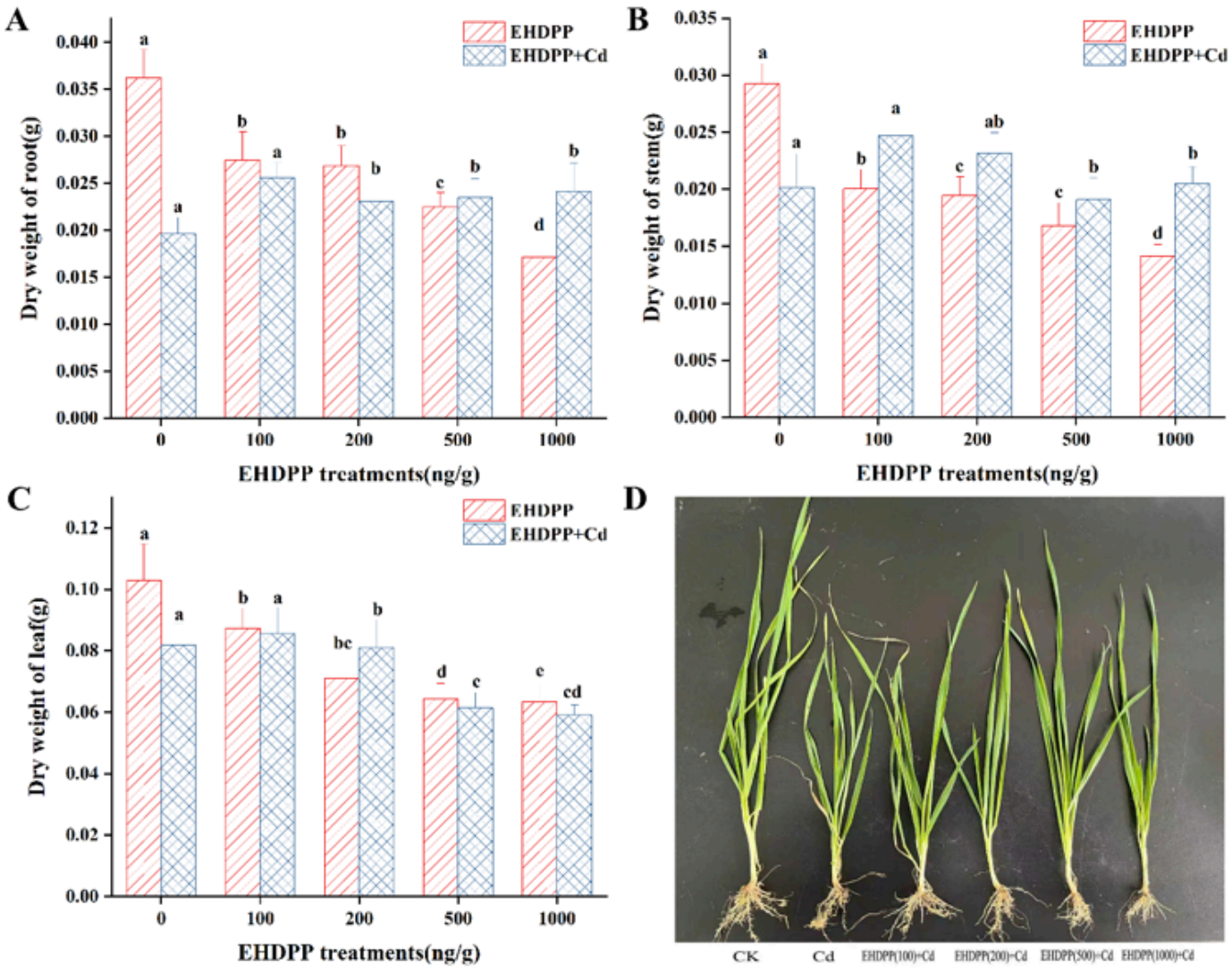


**Figure 1**

Effect of root dry weight (A), stem dry weight (B) and leaf dry weight (C) of wheat under single EHDPP and EHDPP combined with Cd treatment. Notes: Groups with the same colour can be compared in any two sets; different letters indicate a significant difference ($P < 0.05$), and error bars represent standard deviation ($n = 6$).

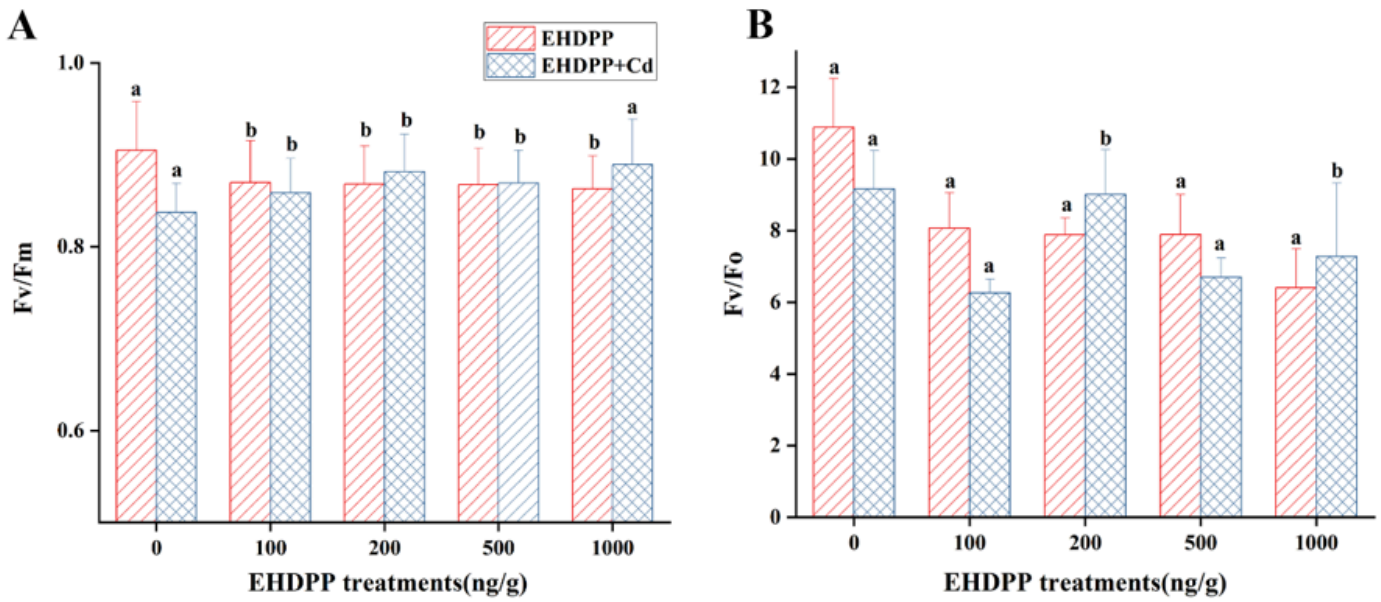


**Figure 2**

$F_v/F_m$ (A) and $F_v/F_0$ (B) of wheat under different treatments. Notes: Groups with the same colour can be compared in any two sets; different letters indicate a significant difference ($P < 0.05$), and error bars represent standard deviation ($n = 3$)

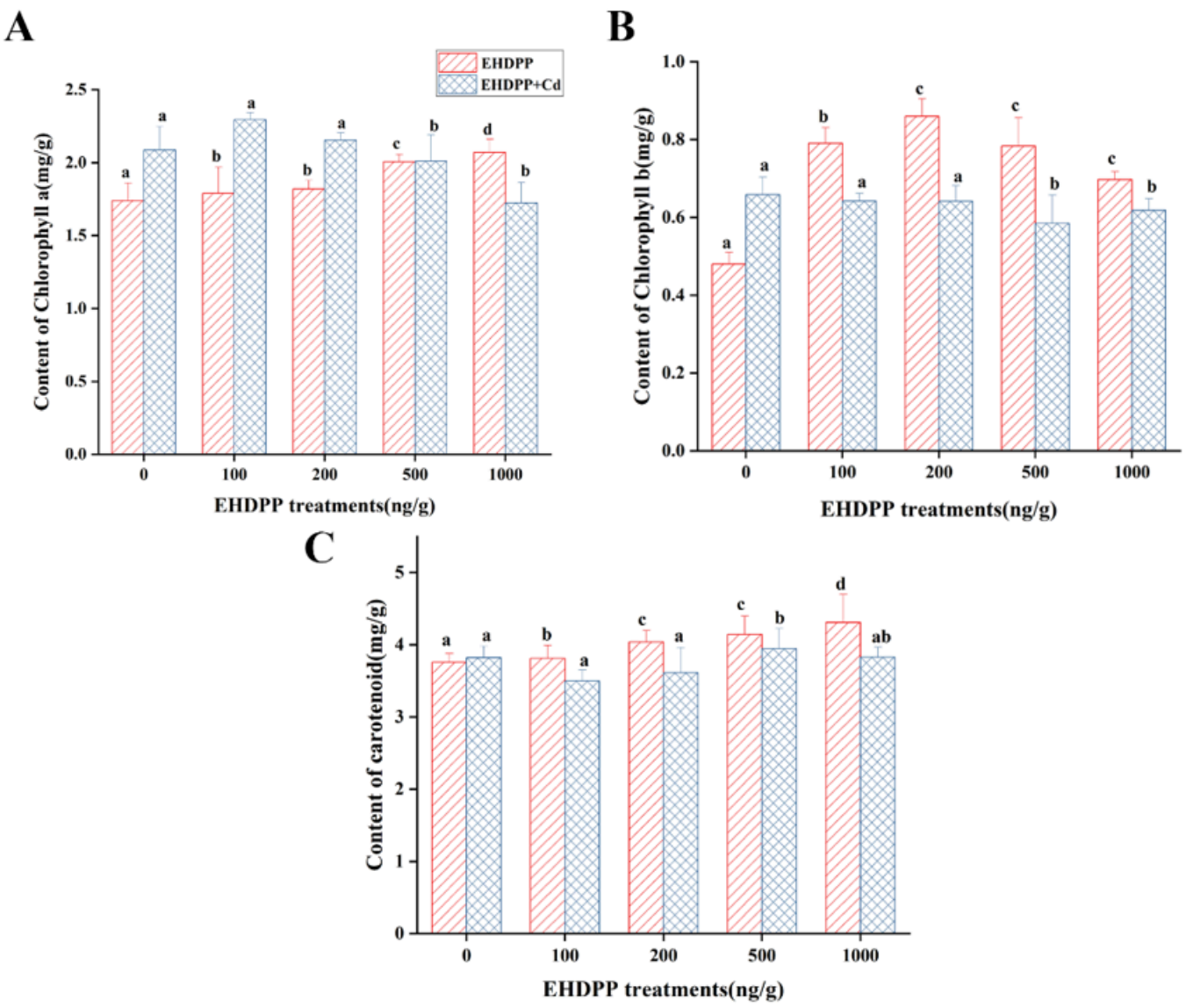


## Figure 3

Effects of single EHDPP and its interaction with cadmium on the contents of chlorophyll a (A), chlorophyll b (B) and carotenoid (C) in wheat. Notes: Groups with the same colour can be compared in any two sets; different letters indicate a significant difference ($P < 0.05$), and error bars represent standard deviation ($n = 3$).

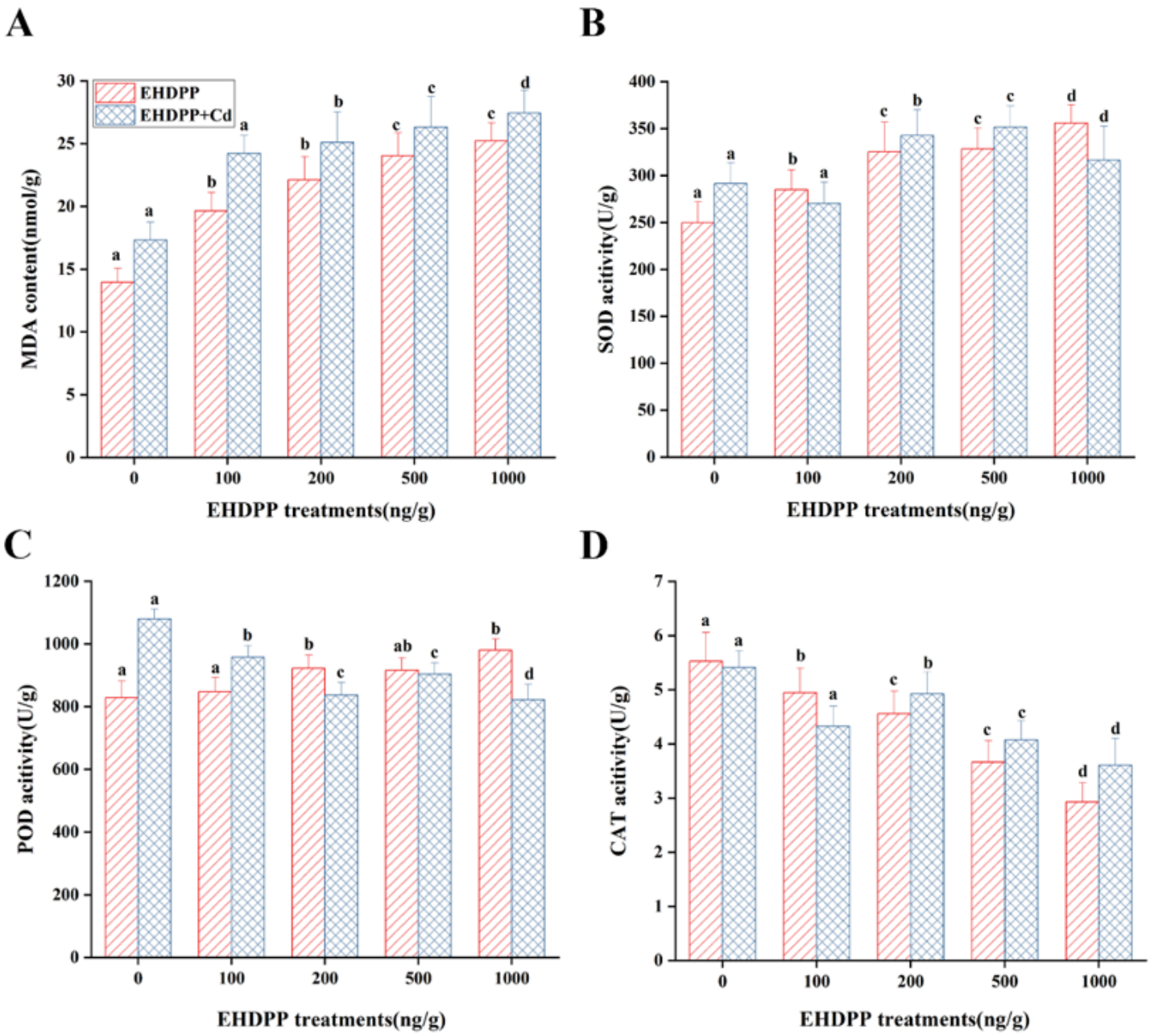


**Figure 4**

Changes of MDA (A), SOD (B), POD (C), and CAT (D) in Wheat under different treatments. Notes: Groups with the same colour can be compared in any two sets; different letters indicate a significant difference ($P < 0.05$), and error bars represent standard deviation ($n = 3$).

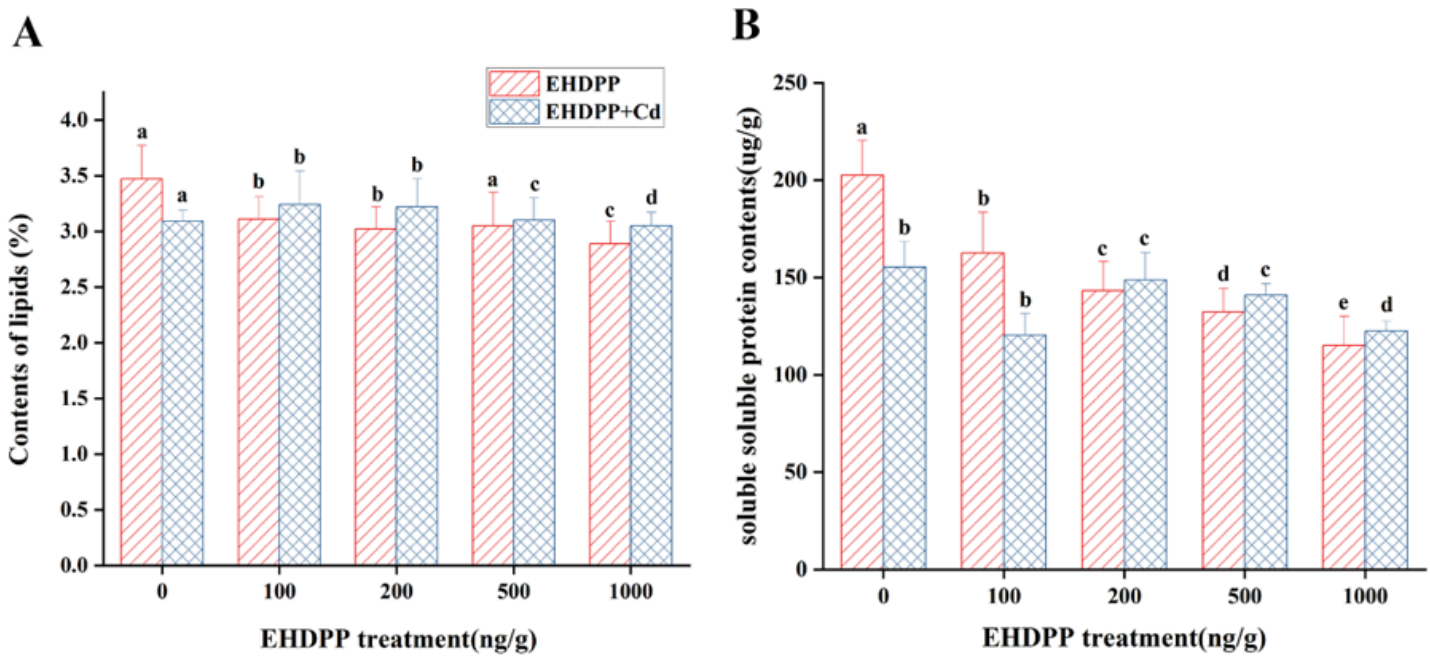


**Figure 5**

Changes in lipid content (A) and soluble protein content (B) of wheat under different treatments. Notes: Groups with the same colour can be compared in any two sets; different letters indicate a significant difference ($P<0.05$), and error bars represent standard deviation (n=3).

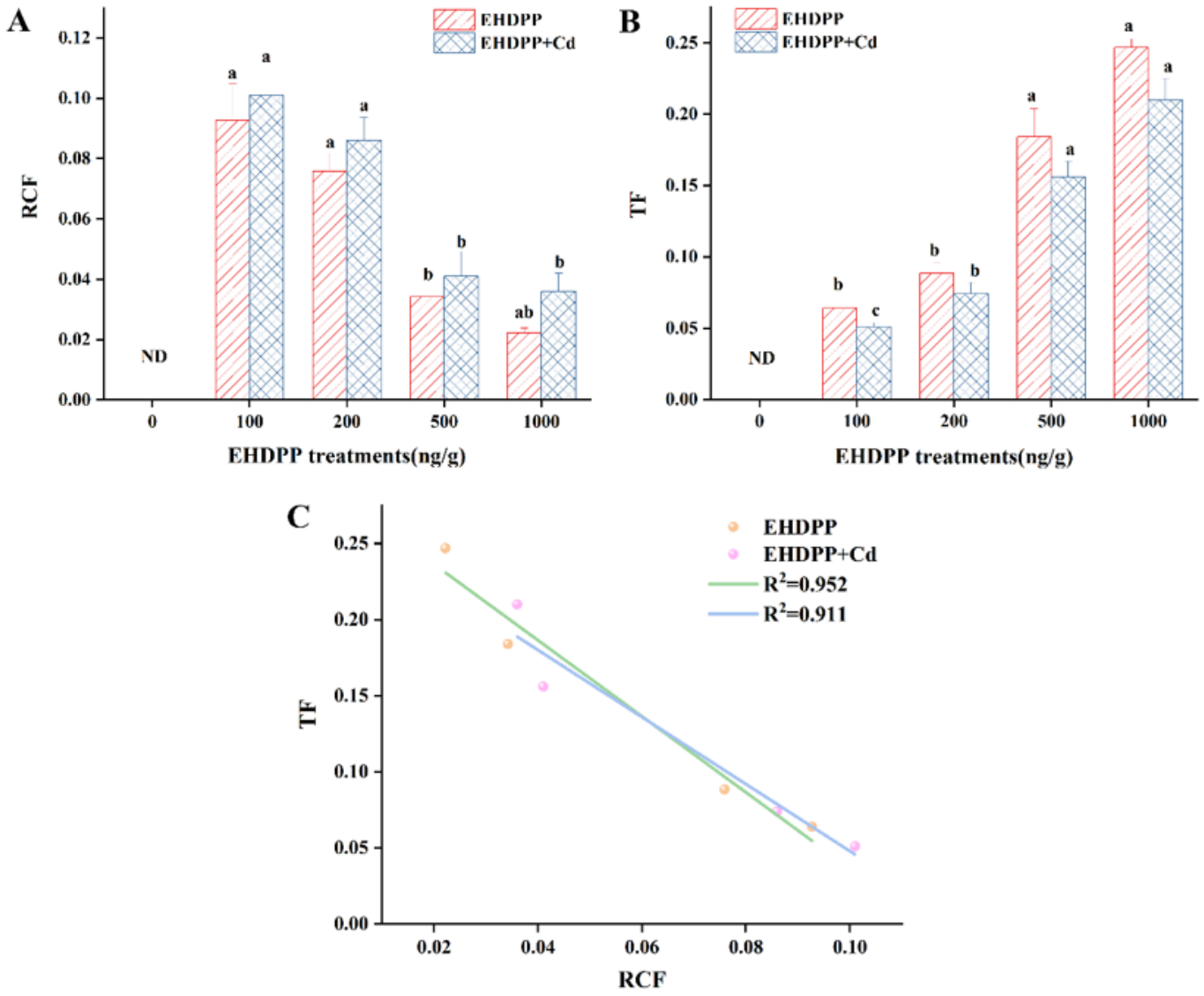


**Figure 6**

RCF and TF of wheat toward EHDPP under different treatments. Notes: Groups with the same colour can be compared in any two sets; different letters indicate a significant difference (P<0.05), and error bars represent standard deviation (n=3).

## Supplementary Files

This is a list of supplementary files associated with this preprint. Click to download.

- Graphicalabstract.png
- SupplementaryMaterial.docx